Inorganic Chemistry Communications 159 (2024) 111810

Contents lists available at ScienceDirect

Inorganic Chemistry Communications

journal homepage: www.elsevier.com/locate/inoche

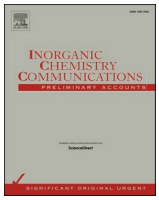

Short communication

Improvement quantum capacitance in supercapacitors using vacancy-defected BC_3 monolayer

Mohamed J. Saadh [a], Chou-Yi Hsu [b,*], M.I. Sayyed [c,d], Anjan Kumar [e], Anmar Ghanim Taki [f], Parminder Singh [g], Ayat Hussein Adhab [h], Yasser Elmasry [i], Sallal A.H. Abdullaha [j]

[a] Faculty of Pharmacy, Middle East University, Amman 11831, Jordan
[b] Department of Pharmacy, Chia Nan University of Pharmacy and Science, Tainan, Taiwan
[c] Department of Physics, Faculty of Science, Isra University, Amman 11622, Jordan
[d] Renewable Energy and Environmental Technology Center, University of Tabuk, Tabuk 47913, Saudi Arabia
[e] Department of Electronics and Communication, GLA University, Mathura 281406, India
[f] Department of Radiology & Sonar Techniques, Al-Noor University College, Nineveh, Iraq
[g] Chemical Engineering Department, Thapar Institute of Engineering and Technology, Patiala, India
[h] Department of Pharmacy, Al-Zahrawi University College, Karbala, Iraq
[i] Department of Mathematics, Faculty of Science, King Khalid University, P.O. Box 9004, Abha 61466, Saudi Arabia
[j] Research Center, Dijlah University College, Baghdad 10022, Iraq

ARTICLE INFO

Keywords:
Supercapacitors
BC_3 monolayer
Quantum capacitance
Vacancy defected

ABSTRACT

In present research, we aimed to assess effectiveness of employing defected BC_3 monolayer in supercapacitors as an electrode through DFT computations. Our focus was on single and double-vacancy BC_3 monolayer. We studied stored charge diagrams, integrated quantum capacitance (C_Q), and density of state (DOS) for both pristine and vacancy-modified defected BC_3 monolayer structures. According to findings, applying vacancy-modified defected structures between −0.80 and 0.80 V leads to greater C_Q value in comparison to pristine BC_3 monolayer. Single and double vacancies may be employed as positive and negative electrodes, and are considered as a semiconductor. Computations reveal that stored charge in vacancy-modified defected structures is more than pristine BC_3 monolayer between 0 and 0.8 V. Moreover, DV-modified defected structure stores more charge than both SV structures and BC_3 monolayer. Our findings suggest that DV BC_3 monolayer shows potential as a material for high-performance supercapacitors.

1. Introduction

Over past decade, demand for portable and compact electronic devices has spurred significant interest in creating sustainable energy storage systems. Despite their widespread use, Li-ion batteries (LIBs) have notable shortcomings such as high maintenance costs, short lifespan, and low power density [1–4]. As an alternative, supercapacitors have gained traction as a promising option due to their inherent advantages, including rapid charging/discharging rates, long cycle life, and remarkable power density [5–11]. At present, the main type of supercapacitor, or electrochemical double-layer capacitor (EDLC), utilizes carbon electrodes adsorbing ions from electrolytes during charging and releasing them upon discharge, thereby allowing for quick and reliable cycles of charge and discharge. The ideal electrode for a supercapacitor should possess several desirable qualities, such as chemical stability to ensure a long lifespan, a large surface area that is easily accessible, strong electrical conductivity, and high specific capacitance. As a result, there have been significant recent efforts focused on developing novel electrode materials and architectures that can improve the performance of supercapacitors [12–14].

For conventional EDLCs, energy storage capabilities are primarily determined by supercapacitor total capacitance (C_T), which is derived from combined contributions of double-layer capacitance (C_D) and electrode quantum capacitance (C_Q). This relationship can be expressed as $1/C_T = 1/C_Q + 1/C_D$ [12,13,15]. Inherent electronic structures of electrode material are the main factor that determines C_Q [16,17], whereas C_D relies on electrode–electrolyte interfacial structure [18–20]. Previous investigations [21–24] have aimed to improve total capacitance by focusing on C_D, achieved by developing porous based materials for electrode with in pore size lower of solvated ions (~1 nm), to

* Corresponding author.
E-mail address: t545316@gmail.com (C.-Y. Hsu).

https://doi.org/10.1016/j.inoche.2023.111810
Received 25 May 2023; Received in revised form 10 October 2023; Accepted 24 November 2023
Available online 25 November 2023

facilitate movement of ions from electrolyte to electrode [25]. Hwang's research group [12] proposed that C_Q is a critical factor in determining total capacitance, leading to considerable efforts being devoted towards enhancing C_Q. Accordingly graphene, which is a 2D hexagonal carbon with sp^2 hybridization, has been extensively studied electrodes [26,27]. According to former reports, practical use of pristine graphene is limited due to low C_Q, which is caused by absence of DOS at Fermi level [28]. Different approaches were proposed to enhance its quantum capacitance, such as utilizing tensile strain and surface rippling [28], introducing vacancies [29], functionalization [30], and chemical doping [31,32].

Due to beneficial characteristics, including thermal stability, low cost, excellent electrical conductivity, and outstanding surface area (2630 m^2 g^{-1}), graphene and its derivatives have been utilized as electrodes [33–37]. Various investigations have shown that modifying graphene through functionalization, introducing defects, and doping or co-doping can be successful approaches for enhancing its C_Q [38]. Introduction of certain substituted groups (e.g. benzene, $–NH_2$, and -H) through functionalization can have a considerable impact on enhancing energy density (*E*) and C_Q of graphene [30,39–41]. According to theoretical studies, Stone Wales, di-interstitials, and di-vacancies defects can enhance C_Q of graphene more than pristine graphene due to presence of quasi-localized states close to Fermi level caused by these defects [42]. To increase C_Q of electrodes made from graphene, dopants, surface rippling, strain, and defects are suggested as effective techniques for modifying carbon-based electrodes [29,43–48]. After analyzing studies on pristine and doped graphene with positive powers, it has been discovered that doped systems deliver favorable characteristics as efficient electrodes [49].

BC3, consisting of a single layer of N and C atoms, shares many similarities with graphene [50–53]. However, it has advantages over graphene, such as a higher-band gap and stronger spin–orbit coupling [54]. The aim of present research was to improve C_Q of BC_3 by introducing vacant areas in monolayer structure. We also sought to optimize the performance of these vacancy-modified BC_3 structures and evaluate their effectiveness as electrodes in supercapacitors. By examining impact of atom vacancies on C_Q and electronic structure of BC_3-based supercapacitors, we aimed to enhance efficacy of electronic storage systems.

2. Computational approach

To conduct DFT computations, GAMESS software has been utilized [55]. Moreover, B3LYP functional was employed that has been augmented with an empirical dispersion term (B3LYP-D) to enhance its accuracy in calculating noncovalent interactions. Previous research has demonstrated that the B3LYP functional is effective in reproducing experimental attributes and has been commonly utilized in investigations of nanostructures [56,57]. Additionally, it has been shown to be a reliable method for calculating III-V semiconductors [58].

To generate stored charge diagrams for both pristine and defected BC_3, integrated quantum capacitance, and gravimetric DOS diagrams, subsequent equations in numerical computations have been employed. C_{total} of electrodes can be represented as below:

$$\frac{1}{C_{total}} = \frac{1}{C_{DL}} + \frac{1}{C_Q} \tag{1}$$

Herein, double-layer capacitance is represented by C_{DL} and quantum capacitance is indicated by C_Q. Total capacity of BC3-based supercapacitors has determined by C_Q rather than C_{DL}. This means that if changes are made to electrode structure that result in an enhancement in C_Q, total capacity of supercapacitor will also increase [12]. Differential quantum capacitance (C_Q^{diff}) is computed as below [59]:

$$C_Q^{diff} = e^2 \int_{-\infty}^{+\infty} D(E) F_T (E - \mu) dE \tag{2}$$

Electrochemical potential μ, expressed by equation $\mu = e\Phi$, where e represents elementary electric charge, can rigidly modify local potential Φ. In Equation (2), relative energy with respect to Fermi level and density of states (1/eV) are represented by E and D(E), respectively. Function of thermal broadening (F_T) is determined as below:

$$F_T = \frac{1}{4k_BT}\left(\frac{E}{2k_BT}\right)$$

Herein, Boltzmann constant is indicated by k_B and temperature is represented by T (300 K). Integrated C_Q (C_Q^{int}) can be computed based on following equation [12,31,60,61]:

$$C_Q^{int} = \frac{1}{V_e} \int_0^V C_Q^{diff}(V') dV'$$

3. Results and discussion

3.1. Electronic and structural attributes of pristine and vacancy-modified BC_3 monolayer

Initially, structural attributes of pristine BC_3 monolayer were optimized and documented. Subsequently, two kinds of vacancies were optimized based on previous investigation: single vacancy (SV) and double vacancy (DV). DOS diagrams for all structures were then computed. Eventually, stored charge diagrams, C_Q^{int}, gravimetric C_Q^{int}, DOS, and gravimetric DOS of both pristine and vacancy-modified BC_3 monolayers were presented.

To analyze electronic and structural attributes of pristine and vacancy-modified defected BC_3 monolayer, optimization has been performed. C-B bond distance was found to be around 1.42 Å, while C—C bond distance was around 1.57 Å. This result was in line with previous experimental and theoretical studies [62]. Pristine BC_3 monolayer had a smaller band gap that was located close to Fermi level. However, presence of defects caused band gap in pristine BC_3 monolayer to increase [51,62].

Two varieties of vacancies or defects were examined over surface of BC_3 monolayer, and it's structures are presented in Fig. 1. Vacancy defects have been investigated widely as a type of point defect, and their effects on physicochemical attributes of nanostructures have been explored [63]. When an atom is lost from a lattice site, a "vacancy" or Schottky defect is created [63]. SV and DV are significant defects that result from a missing atom in their conventional atomic site. It is important to note that vacancies are typically formed during solidification as a result of atoms' vibration and local rearrangement [63]. Band gap values of single and double vacancy of BC_3 were computed, and outcomes were found to be lower than those of pristine BC_3 monolayer. DOS diagrams of vacancy-modified defected BC_3 monolayer are displayed in Fig. 2. Following an enhancement in quantity of absent atoms and enlargement of cavity in BC_3 monolayer, electronic states with lower energy levels were occupied by cavities and electrons. This resulted in a reduction in height of peaks and a shift of diagrams towards conduction band. Maximum peak range for total DOS diagrams increased from 3 to 5 eV. Accordingly, unlike pristine BC_3 monolayer, defected BC_3 monolayer became a p-type semiconductor.

3.2. Computation C_Q of pristine and vacancy-modified BC_3 monolayer

The BC_3 monolayer has potential applications as an electrode in supercapacitors. Former studies have shown that C_Q is linked to DOS that in turn is connected to charge. The Fermi surface energy value in pristine BC_3 is equal to −5.04 electron volts. The Fermi surface energy value in samples with single and double defects is equal to −4.86 and

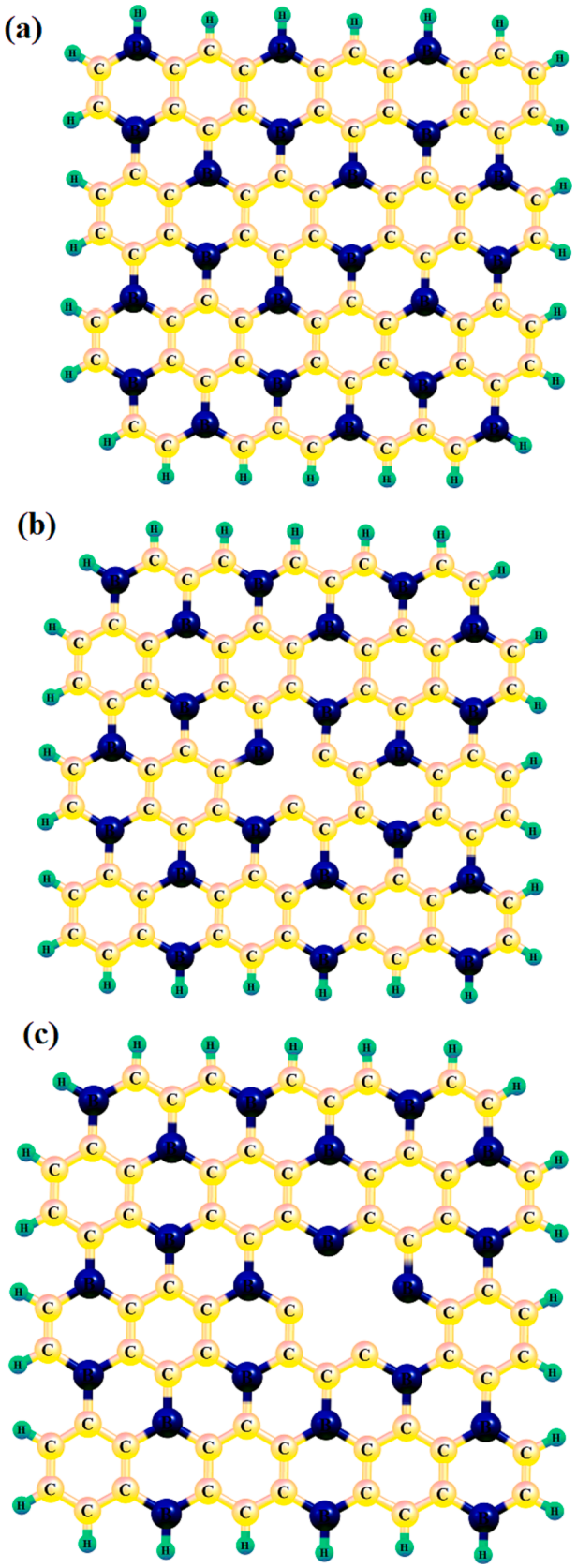

Fig. 1. The proposed BC_3 monolayer models including (a) pristine, (b) single-vacancy, and (c) double-vacancy BC_3 monolayer.

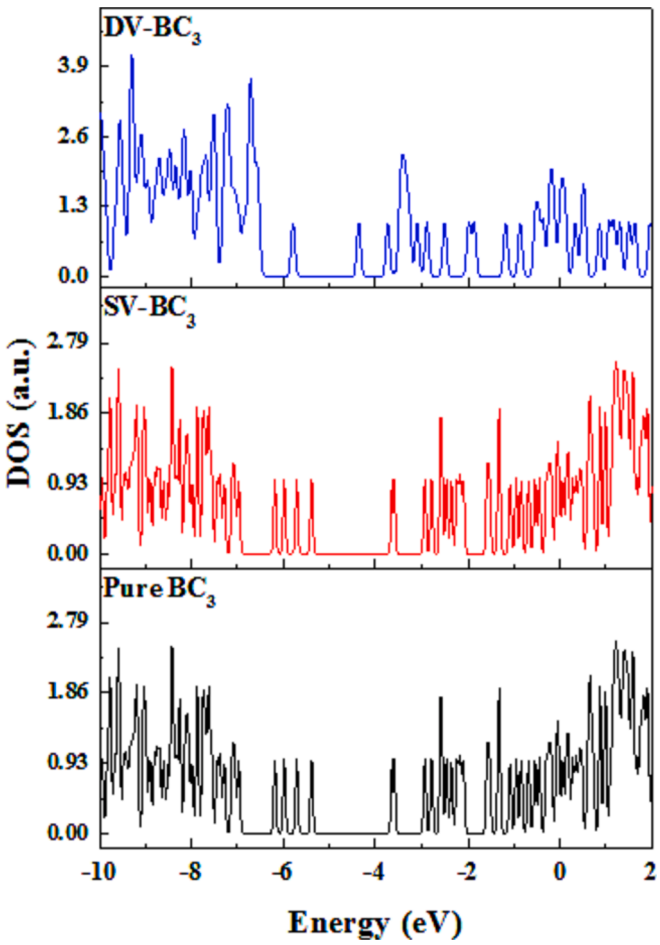

Fig. 2. DOS plots of the (a) pristine, (b) single-vacancy, and (c) double-vacancy BC_3 monolayer.

−4.21 electron volts, respectively. Moreover, Fig. 2 provided an illustration of the total DOS (TDOS) of both unmodified and modified BC_3. It was observed that the bond gap of modified BC_3 (SV = 1.94 eV) and DV = 1.53 eV) was lower than that of BC_3 (2.17 eV), which was a semiconductor. In the case of modified BC_3, certain DOS peaks surpassed the Fermi Level, indicating conductor-like behavior attributed to the presence of unpaired electrons. Yang's research group have indicated that SV defects have a significant impact on improving C_Q of BC_3 monolayer owing to presence of localized states close to Fermi level. Models of SV graphene with varying vacancy concentrations exhibit superior C_Q results compared to pristine graphene. C_Q values (measured in F/cm^2) were noted for two different varieties of DV: (5-8-5) and (555–777). C_Q of structures between −1.50 and 1.50 V is greater than that of bare graphene [64]. Utilizing DFT, it was found that C_Q of SV BC_3 monolayer enhanced owing to attendance of localized states close to Fermi level. Fig. 3 are shown in the gravimetric DOS diagrams for both pristine and vacancies BC_3 monolayer. To obtain DOS, density of states for pristine material can be divided by its molecular weight. Defects in monolayer cause peaks to appear with higher intensity between −0.80 and 0.80 V, as a result of an increase in localized states close to Fermi level. Impurity states observed close to Fermi level in density of states diagrams of defected modified BC_3 were attributed to p orbitals of atoms involved in defect. Enhancement in number of orbitals has a significant impact on altering energy of Fermi level. These impurity states serve as a foundation for enhancing C_{total} and C_Q.

Fig. 4 displays computed C_Q values for pristine BC_3 monolayer and vacancy-modified defected BC_3 monolayer structures (SV and DV) over −0.80 to + 0.80 V (electrochemical range for aqueous electrolytes). As

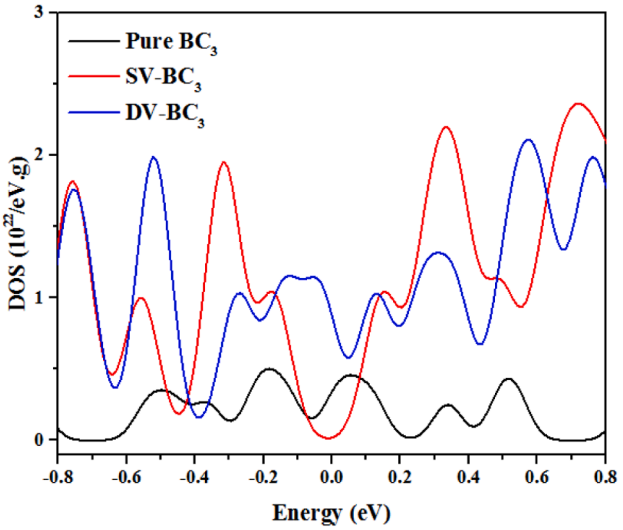

Fig. 3. Gravimetric DOS plots of the (a) pristine, (b) single-vacancy, and (c) double-vacancy BC_3 monolayer.

anticipated, defects altered attributes of pristine BC_3 monolayer structure and had a significant impact on C_Q diagrams, with each structure exhibiting optimal performance at a specific potential. Compared to pristine BC_3 monolayer, vacancy-modified defected BC_3 monolayer structures exhibit asymmetric behaviors, but show a considerable increase in positive and negative potentials within a certain range. Quantum capacitance was found to enhance with an increment in defects concentration and number of missing atoms [65].

Fig. 4 indicates C_Q^{int} values of vacancy-modified defected and pristine BC_3 monolayer. Findings indicate that C_Q of BC_3 monolayer with vacancy modification and defects is greater than pristine BC_3 monolayer within −0.80 to 0.80 V. Compared to pristine BC_3 monolayer at 0 V, quantum capacitance of all structures exhibited enhancement. Upon closer examination, it was observed that CQ value of DV showed a remarkable improvement over other structures at high voltages from 0 to 0.80 V. Based on information obtained from Fig. 4, it can be concluded that DV performs well and can serve as a positive electrode. The amount of charge stored in a BC_3 monolayer, both in its pristine form and with vacancy modification and defects between − 0.80 and + 0.80 V are indicated in Fig. 5. Compared to pristine BC_3 monolayer, capability to store electric charges at positive voltages enhances. As shown in Fig. 4, stored charge diagrams for defect structures exhibit an increment in positive voltages compared to pristine BC_3 monolayer. Comparing different structures, DV exhibits the best performance between 0 and 0.80 V, with a significant increase in stored charge compared to pristine BC_3 monolayer, as shown in Fig. 5. Between −0.80 and 0 V, pristine BC_3 monolayer has a higher stored charge than defective structures. At 0 V, all structures have a stored charge value of 0 V, similar to that of pristine BC_3 monolayer.

4. Conclusion

Density functional theory computations were utilized to explore potential of BC_3 monolayers as electrode materials for supercapacitors. We proposed an approach to increase quantum capacitance of BC_3 by introducing appropriate vacancy defects. The creation of vacancies had a remarkable impact on electronic structure and DOS of BC_3 monolayer. Specifically, the defect resulted in increased energy levels in p molecular orbitals of atoms involved, as well as an increase in total capacitance and available quantum capacitance of supercapacitor. Among the structures investigated, DV configuration showed the most promising results, with a theoretical C_Q value of up to 657 F/g at positive electrode. These findings indicate that vacancy-modified defected BC_3 structures could serve as effective electrode materials for supercapacitors.

Declaration of competing interest

The authors declare that they have no known competing financial interests or personal relationships that could have appeared to influence

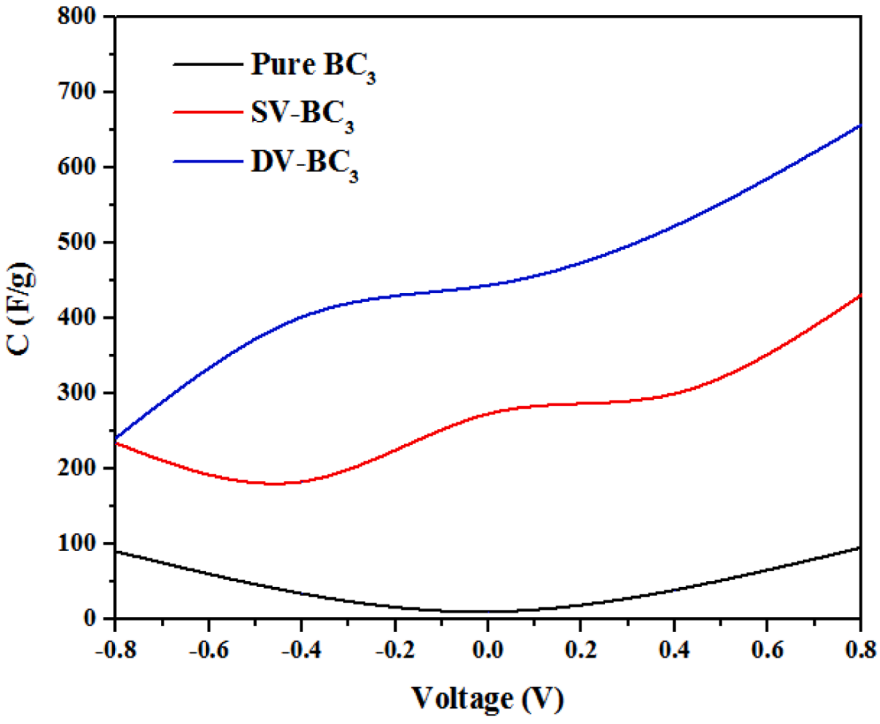

Fig. 4. Integrated quantum capacitance of the pristine, single-vacancy, and double-vacancy BC_3 monolayer.

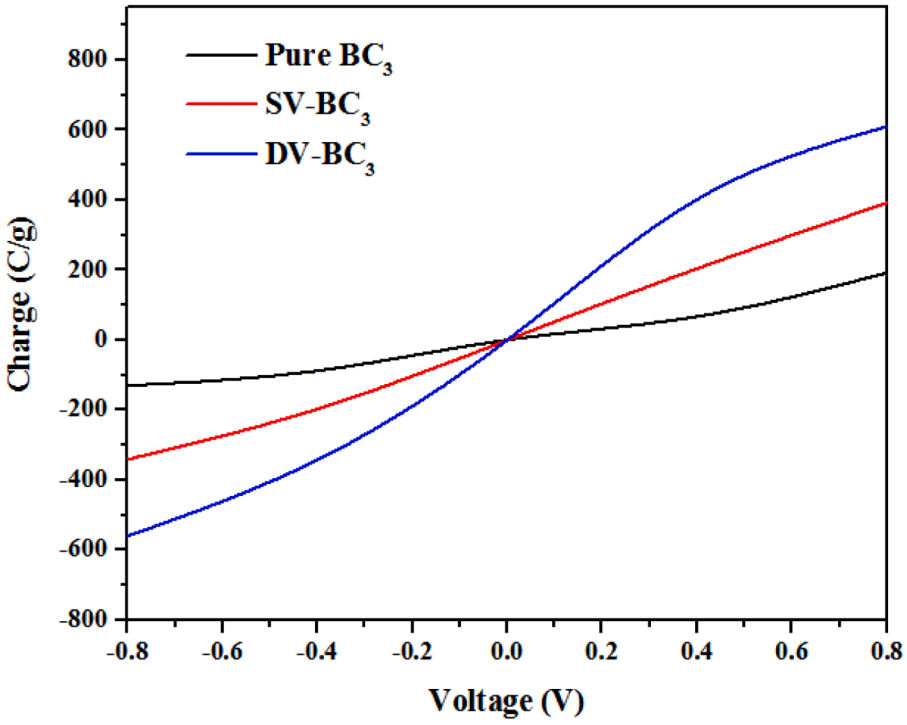

Fig. 5. Calculated stored charge of the pristine, single-vacancy, and double-vacancy BC_3 monolayer.

the work reported in this paper.

Data availability

No data was used for the research described in the article.

Acknowledgments

The authors extend their appreciation to the Deanship of Scientific Research at King Khalid University for funding this work through the Large Groups under grant number (RGP.2/582/44).

References

[1] S. Mu, Q. Liu, P. Kidkhunthod, X. Zhou, W. Wang, Y. Tang, Molecular grafting towards high-fraction active nanodots implanted in N-doped carbon for sodium dual-ion batteries, Natl. Sci. Rev. 8(7) (2020).
[2] D. Xie, M. Zhang, Q. Liu, Y. Lin, A. Yu, Y. Tang, Organic-Inorganic Conformal Extending High-Purity Metal Nanosheets for Robust Electrochemical Lithium-Ion Storage, Adv. Funct. Mater. (2023).
[3] W. Hao, J. Xie, Reducing diffusion-induced stress of bilayer electrode system by introducing pre-strain in lithium-ion battery, J. Electrochem. Energy Convers. Storage 18 (2021), 020909.
[4] J. Xie, X. Wei, X. Bo, P. Zhang, P. Chen, W. Hao, et al., State of charge estimation of lithium-ion battery based on extended Kalman filter algorithm. Frontiers in Energy, Research 11 (2023).
[5] V. Augustyn, P. Simon, B. Dunn, Pseudocapacitive oxide materials for high-rate electrochemical energy storage, Energ. Environ. Sci. 7 (2014) 1597–1614.
[6] M.R. Lukatskaya, B. Dunn, Y. Gogotsi, Multidimensional materials and device architectures for future hybrid energy storage, Nat. Commun. 7 (2016) 1–13.
[7] F. Bonaccorso, L. Colombo, G. Yu, M. Stoller, V. Tozzini, A.C. Ferrari, et al., Graphene, related two-dimensional crystals, and hybrid systems for energy conversion and storage, Science 347 (2015) 1246501.
[8] Y. He, F. Wang, G. Du, L. Pan, K. Wang, R. Gerhard, et al., Revisiting the thermal ageing on the metallised polypropylene film capacitor: From device to dielectric film, High Voltage 8 (2023) 305–314.
[9] L. Kong, Y. Liu, L. Dong, L. Zhang, L. Qiao, W. Wang, et al., Enhanced red luminescence in CaAl 12 O 19: Mn 4+ via doping Ga 3+ for plant growth lighting, Dalton Trans. 49 (2020) 1947–1954.
[10] X. Zhang, Y. Tang, F. Zhang, C.S. Lee, A novel aluminum–graphite dual-ion battery, Adv. Energy Mater. 6 (2016) 1502588.
[11] M. Wang, C. Jiang, S. Zhang, X. Song, Y. Tang, H.-M. Cheng, Reversible calcium alloying enables a practical room-temperature rechargeable calcium-ion battery with a high discharge voltage, Nat. Chem. 10 (2018) 667–672.
[12] E. Paek, A.J. Pak, G.S. Hwang, A computational study of the interfacial structure and capacitance of graphene in [BMIM][PF6] ionic liquid, J. Electrochem. Soc. 160 (2012) A1.
[13] J. Xia, F. Chen, J. Li, N. Tao, Measurement of the quantum capacitance of graphene, Nat. Nanotechnol. 4 (2009) 505–509.
[14] X. Feng, L. Sun, W. Wang, Y. Zhao, J.-W. Shi, Construction of CdS@ ZnO core–shell nanorod arrays by atomic layer deposition for efficient photoelectrochemical H2 evolution, Sep. Purif. Technol. 324 (2023), 124520.
[15] M.D. Stoller, C.W. Magnuson, Y. Zhu, S. Murali, J.W. Suk, R. Piner, et al., Interfacial capacitance of single layer graphene, Energ. Environ. Sci. 4 (2011) 4685–4689.
[16] S. Luryi, Quantum capacitance devices, Appl. Phys. Lett. 52 (1988) 501–503.
[17] A. Das, S. Pisana, B. Chakraborty, S. Piscanec, S.K. Saha, U.V. Waghmare, et al., Monitoring dopants by Raman scattering in an electrochemically top-gated graphene transistor, Nat. Nanotechnol. 3 (2008) 210–215.
[18] Y. Shim, H.J. Kim, Nanoporous carbon supercapacitors in an ionic liquid: a computer simulation study, ACS Nano 4 (2010) 2345–2355.
[19] J. Huang, B.G. Sumpter, V. Meunier, A universal model for nanoporous carbon supercapacitors applicable to diverse pore regimes, carbon materials, and electrolytes, Chem.– Eur. J. 14 (2008) 6614–6626.
[20] G. Feng, P.T. Cummings, Supercapacitor capacitance exhibits oscillatory behavior as a function of nanopore size, J. Phys. Chem. Lett.. 2 (2011) 2859–2864.
[21] E. Frackowiak, F. Beguin, Carbon materials for the electrochemical storage of energy in capacitors, Carbon 39 (2001) 937–950.
[22] A. Jänes, L. Permann, M. Arulepp, E. Lust, Electrochemical characteristics of nanoporous carbide-derived carbon materials in non-aqueous electrolyte solutions, Electrochem. Commun. 6 (2004) 313–318.
[23] C. Largeot, C. Portet, J. Chmiola, P.-L. Taberna, Y. Gogotsi, P. Simon, Relation between the ion size and pore size for an electric double-layer capacitor, J. Am. Chem. Soc. 130 (2008) 2730–2731.
[24] J. Chmiola, C. Largeot, P.L. Taberna, P. Simon, Y. Gogotsi, Desolvation of ions in subnanometer pores and its effect on capacitance and double-layer theory, Angew. Chem. Int. Ed. 47 (2008) 3392–3395.
[25] J. Chmiola, G. Yushin, Y. Gogotsi, C. Portet, P. Simon, P.-L. Taberna, Anomalous increase in carbon capacitance at pore sizes less than 1 nanometer, Science 313 (2006) 1760–1763.
[26] P. Hirunsit, M. Liangruksa, P. Khanchaitit, Electronic structures and quantum capacitance of monolayer and multilayer graphenes influenced by Al, B, N and P doping, and monovacancy: Theoretical study, Carbon 108 (2016) 7–20.
[27] B. Liu, X. Wang, Y. Chen, H. Xie, X. Zhao, A.B. Nassr, et al., Honeycomb carbon obtained from coal liquefaction residual asphaltene for high-performance supercapacitors in ionic and organic liquid-based electrolytes, J. Storage Mater. 68 (2023), 107826.

[28] B.C. Wood, T. Ogitsu, M. Otani, J. Biener, First-Principles-Inspired Design Strategies for Graphene-Based Supercapacitor Electrodes, J. Phys. Chem. C 118 (2014) 4–15.
[29] G. Yang, H. Zhang, X. Fan, W. Zheng, Density functional theory calculations for the quantum capacitance performance of graphene-based electrode material, J. Phys. Chem. C 119 (2015) 6464–6470.
[30] S.M. Mousavi-Khoshdel, E. Targholi, Exploring the effect of functionalization of graphene on the quantum capacitance by first principle study, Carbon 89 (2015) 148–160.
[31] E. Paek, A.J. Pak, K.E. Kweon, G.S. Hwang, On the origin of the enhanced supercapacitor performance of nitrogen-doped graphene, J. Phys. Chem. C 117 (2013) 5610–5616.
[32] R. Ren, F. Lai, X. Lang, L. Li, C. Yao, K. Cai, Efficient sulfur host based on Sn doping to construct Fe2O3 nanospheres with high active interface structure for lithium-sulfur batteries, Appl. Surf. Sci. 613 (2023), 156003.
[33] Y. Zhai, Y. Dou, D. Zhao, P.F. Fulvio, R.T. Mayes, S. Dai, Carbon materials for chemical capacitive energy storage, Adv. Mater. 23 (2011) 4828–4850.
[34] S. Vivekchand, C.S. Rout, K. Subrahmanyam, A. Govindaraj, C.N.R. Rao, Graphene-based electrochemical supercapacitors, J. Chem. Sci. 120 (2008) 9–13.
[35] J.J. Yoo, K. Balakrishnan, J. Huang, V. Meunier, B.G. Sumpter, A. Srivastava, et al., Ultrathin planar graphene supercapacitors, Nano Lett. 11 (2011) 1423–1427.
[36] X.-H. Li, S.-S. Li, X.-H. Cui, R.-Z. Zhang, H.-L. Cui, First-principle study of electronic properties and quantum capacitance of lithium adsorption on pristine and vacancy-defected O-functionalized Ti2C MXene, Appl. Surf. Sci. 563 (2021), 150264.
[37] J. Luo, H. Han, X. Wang, X. Qiu, B. Liu, Y. Lai, et al., Single-atom Nb anchored on graphitic carbon nitride for boosting electron transfer towards improved photocatalytic performance, Appl Catal B 328 (2023), 122495.
[38] Q. Xu, G. Yang, X. Fan, W. Zheng, Improving the quantum capacitance of graphene-based supercapacitors by the doping and co-doping: first-principles calculations, ACS Omega 4 (2019) 13209–13217.
[39] Z. Lin, Y. Liu, Y. Yao, O.J. Hildreth, Z. Li, K. Moon, et al., Superior capacitance of functionalized graphene, J. Phys. Chem. C 115 (2011) 7120–7125.
[40] T. Sruthi, T. Kartick, Route to achieving enhanced quantum capacitance in functionalized graphene based supercapacitor electrodes, J. Phys. Condens. Matter 31 (2019), 475502.
[41] T, S., Devaraj, N., Tarafder, K. Theoretical investigation of quantum capacitance in the functionalized MoS2-monolayer. Electronic Structure. 2021, 3, 025003.
[42] A.J. Pak, E. Paek, G.S. Hwang, Tailoring the performance of graphene-based supercapacitors using topological defects: A theoretical assessment, Carbon 68 (2014) 734–741.
[43] J. Rihm, E.S. Sim, S.B. Cho, Y.-C. Chung, Enhancement of the quantum capacitances of group-14 elemental two-dimensional materials by Ti-doping: A first principles study, Appl. Surf. Sci. 530 (2020), 147301.
[44] G.S. Kliros, Strain effects on the quantum capacitance of graphene nanoribbon devices, Appl. Surf. Sci. 502 (2020), 144292.
[45] E. Paek, A.J. Pak, G.S. Hwang, Large capacitance enhancement induced by metal-doping in graphene-based supercapacitors: a first-principles-based assessment, ACS Appl. Mater. Interfaces 6 (2014) 12168–12176.
[46] Q. Cheng, J. Tang, J. Ma, H. Zhang, N. Shinya, L.-C. Qin, Graphene and carbon nanotube composite electrodes for supercapacitors with ultra-high energy density, PCCP 13 (2011) 17615–17624.
[47] Q. Zhou, L. Wang, W. Ju, Y. Yong, S. Wu, S. Cai, et al., Quantum capacitance of vacancy-defected and co-doped stanene for supercapacitor electrodes: A theoretical study, Electrochim. Acta 433 (2022), 141261.
[48] C. Lu, H. Zhou, L. Li, A. Yang, C. Xu, Z. Ou, et al., Split-core magnetoelectric current sensor and wireless current measurement application, Measurement 188 (2022), 110527.
[49] M. Mousavi-Khoshdel, E. Targholi, M.J. Momeni, First-principles calculation of quantum capacitance of codoped graphenes as supercapacitor electrodes, J. Phys. Chem. C 119 (2015) 26290–26295.
[50] H. Zhang, Y. Liao, G. Yang, X. Zhou, Theoretical studies on the electronic and optical properties of honeycomb BC3 monolayer: a promising candidate for metal-free photocatalysts, ACS Omega 3 (2018) 10517–10525.
[51] S. Thomas, A.K. Madam, M.A. Zaeem, Stone–wales defect induced performance improvement of BC3 monolayer for high capacity lithium-ion rechargeable battery anode applications, J. Phys. Chem. C 124 (2020) 5910–5919.
[52] Y. Wang, N. Zhou, Y. Li, Electrochemical catalytic mechanism of single transition metal atom embedded BC3 monolayer for oxygen reduction and evolution reactions, Chem. Eng. J. 425 (2021), 130631.
[53] F. Yu, S. Yu, C. Li, Z. Li, F. Song, Z. Xu, et al., Molecular engineering of biomimetic donor-acceptor conjugated microporous polymers with full-spectrum response and an unusual electronic shuttle for enhanced uranium (VI) photoreduction, Chem. Eng. J. 466 (2023), 143285.
[54] Y. Li, T. Hussain, A. De Sarkar, R. Ahuja, Hydrogen storage in polylithiated BC3 monolayer sheet, Solid State Commun. 170 (2013) 39–43.
[55] M.W. Schmidt, K.K. Baldridge, J.A. Boatz, S.T. Elbert, M.S. Gordon, J.H. Jensen, et al., General atomic and molecular electronic structure system, J. Comput. Chem. 14 (1993) 1347–1363.
[56] J. Beheshtian, A.A. Peyghan, Z. Bagheri, Detection of phosgene by Sc-doped BN nanotubes: a DFT study, Sens. Actuators B 171 (2012) 846–852.
[57] M.A. Abdulsattar, SiGe superlattice nanocrystal pure and doped with substitutional phosphorus single atom: Density functional theory study, Superlattice. Microst. 50 (2011) 377–385.
[58] S. Tomić, B. Montanari, N. Harrison, The group III–V's semiconductor energy gaps predicted using the B3LYP hybrid functional, Physica E 40 (2008) 2125–2127.
[59] T. Fang, A. Konar, H. Xing, D. Jena, Carrier statistics and quantum capacitance of graphene sheets and ribbons, Appl. Phys. Lett. 91 (2007), 092109.
[60] D. John, L. Castro, D. Pulfrey, Quantum capacitance in nanoscale device modeling, J. Appl. Phys. 96 (2004) 5180–5184.
[61] J.P. Selvaggi, A general analytical method for finding the quantum capacitance of graphene, J. Comput. Electron. 17 (2018) 1268–1275.
[62] A. Bafekry, S. Farjami Shayesteh, M. Ghergherehchi, F.M. Peeters, Tuning the bandgap and introducing magnetism into monolayer BC3 by strain/defect engineering and adatom/molecule adsorption, J. Appl. Phys. 126 (2019), 144304.
[63] B. Pan, W. Yang, J. Yang, Formation energies of topological defects in carbon nanotubes, Phys. Rev. B 62 (2000) 12652.
[64] S.M. Seyed-Talebi, J. Beheshtian, M. Neek-Amal, Doping effect on the adsorption of NH3 molecule onto graphene quantum dot: From the physisorption to the chemisorption, J. Appl. Phys. 114 (2013), 124307.
[65] G. Yang, Q. Xu, X. Fan, W. Zheng, Quantum capacitance of silicene-based electrodes from first-principles calculations, J. Phys. Chem. C 122 (2018) 1903–1912.